



# Contributions to SAR Image Time Series Analysis

---

**Ammar Mian**

Ph.d defense - 26 September 2019

**Supervisors:** Jean-Philippe Ovarlez (ONERA & SONDRA),  
Guillaume Ginolhac (LISTIC)  
and Abdourahmane M. Atto (LISTIC)



# Contents of the presentation

## 1 Introduction

- Motivations
- Data

## 2 Change detection based on a statistical framework

- The problem
- State of the art

## 3 Robust Covariance homogeneity testing for Change Detection

- Tests using Complex Elliptical Symmetric distributions
- Tests using deterministic compound-Gaussian modelling

## 4 Tests using Low-rank models

## 5 Clustering SAR ITS with Riemannian geometry: an opening

## 6 Conclusions

# Contents of the presentation

## 1 Introduction

- Motivations
- Data

## 2 Change detection based on a statistical framework

- The problem
- State of the art

## 3 Robust Covariance homogeneity testing for Change Detection

- Tests using Complex Elliptical Symmetric distributions
- Tests using deterministic compound-Gaussian modelling

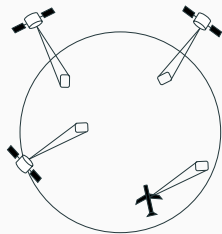
## 4 Tests using Low-rank models

## 5 Clustering SAR ITS with Riemannian geometry: an opening

## 6 Conclusions

# Remote Sensing: big data analysis

Remote sensing allows to obtain image of the Earth's surface for various applications such as **Change Detection**.



Huge increase in the number of available acquisitions:

- Sentinel-1: 12 days repeat cycle, since 2014
- TerraSAR-X: 11 days repeat cycle, since 2007
- UAVSAR, ... thousands of flight paths planned

## Problem

→ There is a need to process the huge amount of data automatically !

# SAR Image Time Series: changes analysis

Change detection is useful for various purposes: Activity monitoring

**Figure 1:** Terrasar-X images of the Burning-man festival

Ph.d defense Ammar Mian, 26 September 2019

# SAR Image Time Series: changes analysis

Change detection is useful for various purposes: Disaster assessment

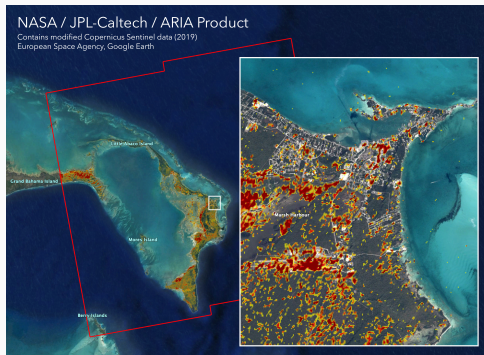
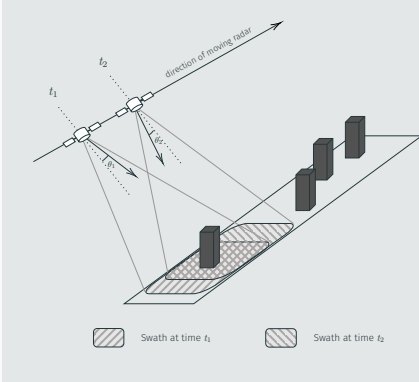


**Figure 1:** Destruction map of Dorian Hurricane in the Bahamas using Change Detection over Sentinel-1 data

# Synthetic aperture radar (SAR)

## Principle of SAR



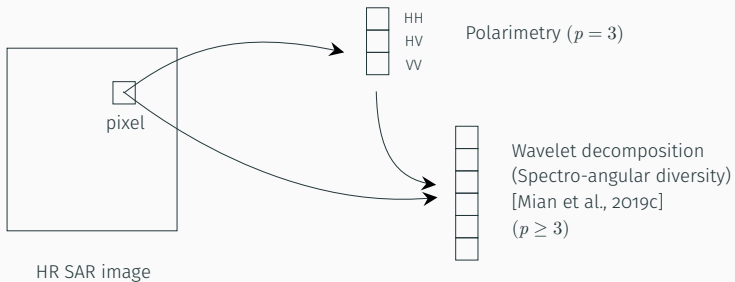
## Advantages:

- All weather and illumination conditions (active technology)
- Very high-resolution (sub-meter) imaging



Comparison of optical and image

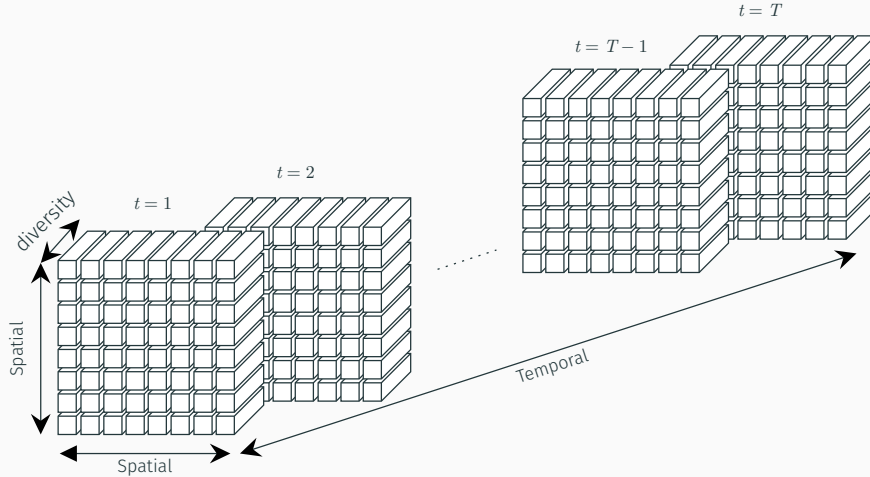
# Multivariate data: natural or pre-processing



## Feature selection

- Leverage **diversity** to improve the detection
- Requires to process **multivariate** pixels

# Data dimensionality



# Non-Gaussianity of HR Images

**Issue:** Data is *non-Gaussian* !

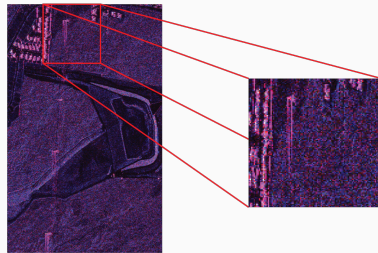
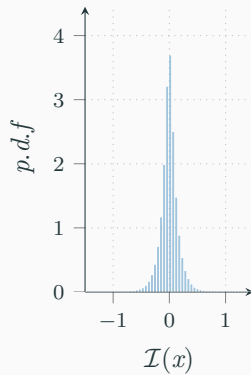
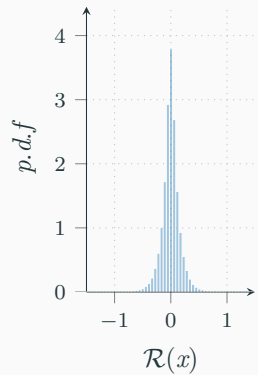
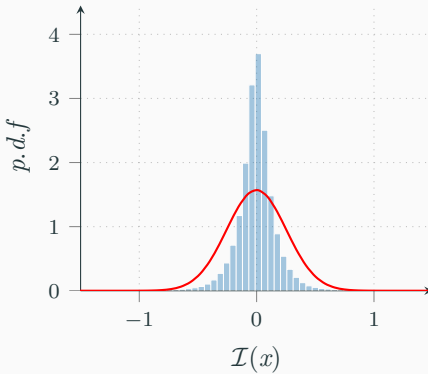
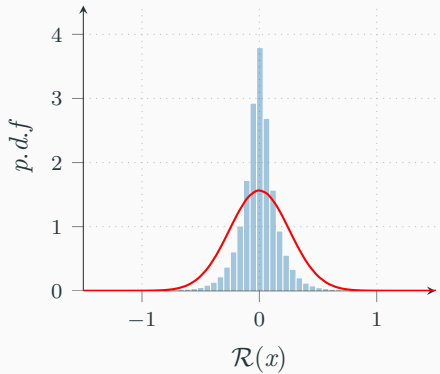


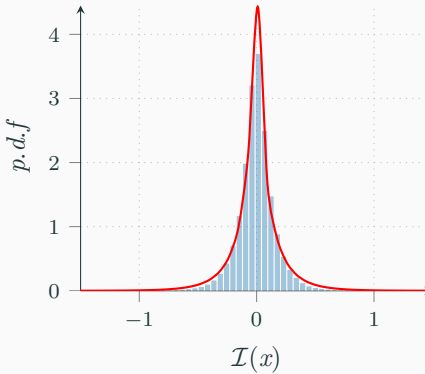
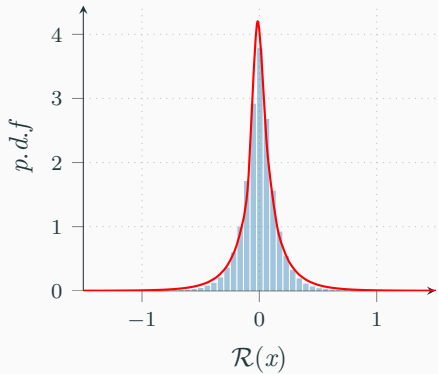
**Figure 2:** UAVSAR data (Courtesy NASA/JPL-Caltech)



# Gaussian distribution fitting



# Generalized Gaussian distribution fitting



# Summary

In the context of this Ph.D we develop change detection methodologies which:

- leverage **diversity** in order to improve detection  
→ It can be obtained through *wavelet transforms* Chapter 2
- take into account the heterogeneity of HR SAR images  
→ We develop methodologies that are **robust to non-Gaussianity** **Chapter 3**

We also consider alternative problems to bring more information:

- about the time at which changes occur  
→ Change-point detection problem Chapter 4
- change patterns  
→ Clustering problem **Chapter 5**

# Contents of the presentation

## 1 Introduction

- Motivations
- Data

## 2 Change detection based on a statistical framework

- The problem
- State of the art

## 3 Robust Covariance homogeneity testing for Change Detection

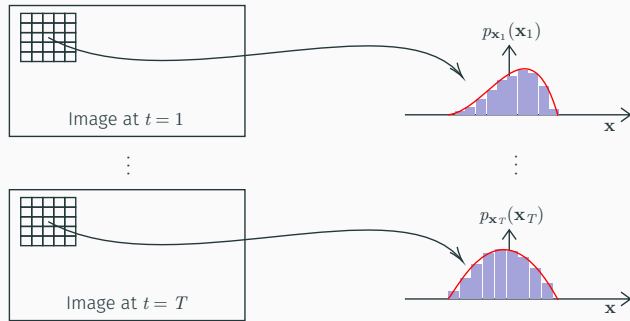
- Tests using Complex Elliptical Symmetric distributions
- Tests using deterministic compound-Gaussian modelling

## 4 Tests using Low-rank models

## 5 Clustering SAR ITS with Riemannian geometry: an opening

## 6 Conclusions

# Statistical framework: principle



## Interest of this approach

- Can account for physical modelling of the data/noise
- Strong theoretical guarantees from statistical litterature

# SAR image time series representation

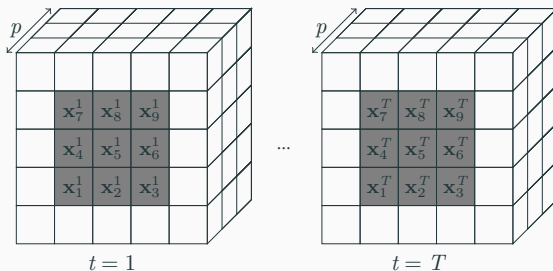


**Figure 3:** Sliding windows  $\mathbb{W}_{1,T}$

$p$	$N$	$T$
dimension of vectors	number of pixels on local window	number of dates in the time series

# Parametric change detection

A probability model is assigned to the observations on the windows over time:

$$\mathbf{x}_k^t \sim p_{\mathbf{x}_k^t}(\mathbf{x}_k^t; \boldsymbol{\theta}_t; \boldsymbol{\Phi}_t).$$

The detection is done on some *parameters of interest*  $\boldsymbol{\theta}_t$  while the remaining ones are the *nuisance parameters*  $\boldsymbol{\Phi}_t$ :

$$\begin{cases} H_0 : \boldsymbol{\theta}_1 = \dots = \boldsymbol{\theta}_T = \boldsymbol{\theta}_0 & \& \boldsymbol{\Phi}_1 \neq \dots \neq \boldsymbol{\Phi}_T, \\ H_1 : \exists (t, t') \in \llbracket 1, T \rrbracket^2, \boldsymbol{\theta}_t \neq \boldsymbol{\theta}_{t'} & \& \boldsymbol{\Phi}_1 \neq \dots \neq \boldsymbol{\Phi}_T \end{cases}. \quad (1)$$

## Problems

- Specify a model and parameters of interest which are
  - A good fit to the empirical distribution
  - Robust to a large class of distributions and outliers
- Find a test statistic to obtain a rule of decision between the two alternatives.

# Test statistic

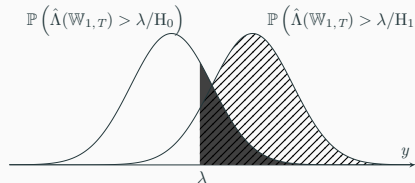
We want to obtain:

- a statistic of decision  $\hat{\Lambda}$ :
- a threshold  $\lambda$

$$\mathbb{C}^{p \times N} \times \cdots \times \mathbb{C}^{p \times N} \rightarrow \mathbb{R}$$
$$\mathbb{W}_{1,T} \rightarrow \hat{\Lambda}(\mathbb{W}_{1,T})$$

## So that

$\mathbb{P}(\hat{\Lambda}(\mathbb{W}_{1,T}) > \lambda/H_1)$  is high while  $\mathbb{P}(\hat{\Lambda}(\mathbb{W}_{1,T}) > \lambda/H_0)$  is low.



# Constant False Alarm Rate (CFAR) property

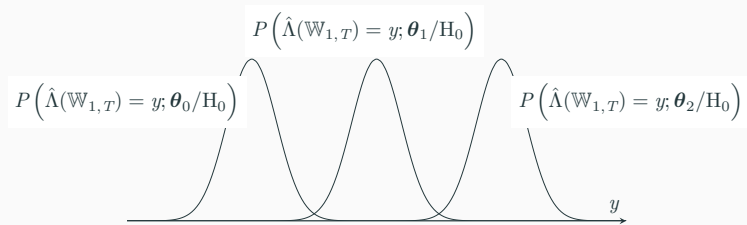
Assume a parametric model:  $\forall k, \forall t, \mathbf{x}_k^t \sim p_{\mathbf{x};\boldsymbol{\theta}}(\mathbf{x}; \boldsymbol{\theta})$ .

## Definition

A statistic  $\hat{\Lambda}$  is said to be CFAR if for any set  $(\boldsymbol{\theta}_0, \boldsymbol{\theta}_1)$ , we have:

$$\mathbb{P}(\hat{\Lambda}(\mathbb{W}_{1,T}; \boldsymbol{\theta}_0 / H_0) = x) = \mathbb{P}(\hat{\Lambda}(\mathbb{W}_{1,T}; \boldsymbol{\theta}_1 / H_0) = x)$$

Example of a non CFAR statistic:



# Generalized Likelihood Ratio Test

Given the change detection decision problem, the GLRT is formulated as follows:

$$\hat{\Lambda} = \frac{\max_{\boldsymbol{\theta}_1, \dots, \boldsymbol{\theta}_T, \Phi_1, \dots, \Phi_T} p_{\mathbb{W}_{1,T}}(\mathbb{W}_{1,T}/H_1; \boldsymbol{\theta}_1, \dots, \boldsymbol{\theta}_T, \Phi_1, \dots, \Phi_T)}{\max_{\boldsymbol{\theta}_0, \Phi_1, \dots, \Phi_T} p_{\mathbb{W}_{1,T}}(\mathbb{W}_{1,T}/H_0; \boldsymbol{\theta}_0, \Phi_1, \dots, \Phi_T)} \stackrel{H_1}{\gtrless} \lambda. \quad (2)$$

→ Good invariance properties [Kay and Gabriel, 2003].

# Gaussian modelling

## Definition

A vector  $\mathbf{x} \in \mathbb{C}^p$  is said to Gaussian distributed with mean parameter  $\boldsymbol{\mu} \in \mathbb{C}^p$  and covariance parameter  $\boldsymbol{\Sigma} \in \mathbb{S}_{\mathbb{H}}^p$ , denoted  $\mathbf{x} \sim \mathbb{C}\mathcal{N}(\boldsymbol{\mu}, \boldsymbol{\Sigma})$  if the Probability Distribution Function (PDF) of its distribution is the following:

$$p_{\mathbf{x}}(\mathbf{x}; \boldsymbol{\mu}, \boldsymbol{\Sigma}) = \frac{1}{\pi^p |\boldsymbol{\Sigma}|^{-1}} \exp \left\{ -(\mathbf{x} - \boldsymbol{\mu})^H \boldsymbol{\Sigma}^{-1} (\mathbf{x} - \boldsymbol{\mu}) \right\}. \quad (3)$$

Introduced by [Conradsen et al., 2003] which is a reference in the domain. The data is modelled by a Gaussian model as follows:

$$\mathbf{x}_k^t \sim \mathbb{C}\mathcal{N}(\mathbf{0}_p, \boldsymbol{\Sigma}_t).$$

Detection test:  $\boldsymbol{\theta}_t = \boldsymbol{\Sigma}_t \quad \& \quad \Phi_t = \emptyset$

# Prior works in Gaussian context

We have the following test:<sup>1</sup>:

## GLRT for covariance homogeneity test in Gaussian context

$$\hat{\Lambda}_G = \frac{\left| \frac{1}{T} \sum_{t=1}^T \hat{\Sigma}_t \right|^{TN}}{\prod_{t=1}^T \left| \hat{\Sigma}_t \right|^N} \stackrel{H_1}{\gtrless} \lambda \quad (4)$$

where  $\forall t$ ,  $\hat{\Sigma}_t = \frac{1}{N} \sum_{k=1}^N \mathbf{x}_k^t (\mathbf{x}_k^t)^H$ .

---

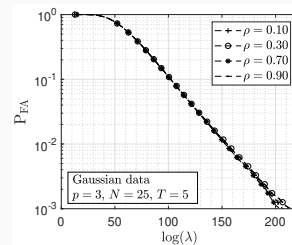
<sup>1</sup>Many other statistics based on other principles exist as described in [Ciuonzo et al., 2017].

# Some properties of the statistic

## CFARness property

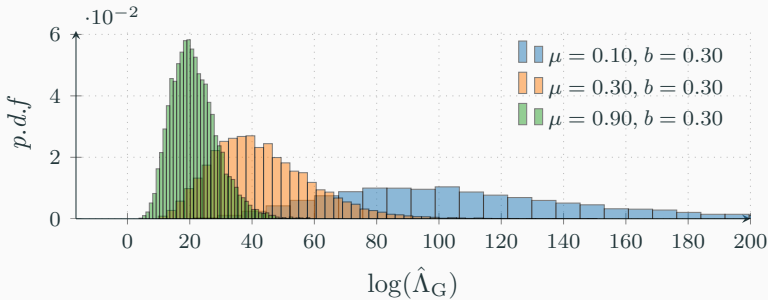
The GLRT statistic is CFAR towards the covariance parameter.

In simulation:  $\mathbf{x}_k^t \sim \mathcal{CN}(\mathbf{0}_p, (\rho^{|i-j|})_{ij})$  with  $10^5$  Monte-Carlo trials.



## Non CFAR behaviour in non-Gaussian context: Experimental results

**In simulation:**  $\mathbf{x}_k^t = \sqrt{\tau_k^t} \mathbf{z}_k^t$  where  $\mathbf{z}_k^t \sim \mathcal{CN}(\mathbf{0}_p, (0.5^{|i-j|})_{ij})$  and  $\tau_k^t \sim \Gamma(\mu, b)$  with  $p = 3$ ,  $N = 10$ ,  $T = 3 \cdot 10^4$  Monte-Carlo trials.



→ The Gaussian GLRT is **not CFAR** in the context of compound-Gaussian distributions !

# Contents of the presentation

## 1 Introduction

- Motivations
- Data

## 2 Change detection based on a statistical framework

- The problem
- State of the art

## 3 Robust Covariance homogeneity testing for Change Detection

- Tests using Complex Elliptical Symmetric distributions
- Tests using deterministic compound-Gaussian modelling

## 4 Tests using Low-rank models

## 5 Clustering SAR ITS with Riemannian geometry: an opening

## 6 Conclusions

# Complex Elliptical Symmetric modelling

## Definition

A vector  $\mathbf{x} \in \mathbb{C}^p$  is said to be Complex Elliptical Symmetric (CES) distributed with density generator function  $g : \mathbb{R}^+ \rightarrow \mathbb{R}^+$ , mean parameter  $\boldsymbol{\mu} \in \mathbb{C}^p$  and scatter matrix parameter  $\boldsymbol{\Sigma} \in \mathbb{S}_{\mathbb{H}}^p$ , denoted  $\mathbf{x} \sim \mathbb{CE}(g, \boldsymbol{\mu}, \boldsymbol{\Sigma})$  if its PDF is of the following form:

$$p_{\mathbf{x}}(\mathbf{x}; g, \boldsymbol{\mu}, \boldsymbol{\Sigma}) = \mathfrak{C}_{p,g} |\boldsymbol{\Sigma}|^{-1} g \left\{ (\mathbf{x} - \boldsymbol{\mu})^H \boldsymbol{\Sigma}^{-1} (\mathbf{x} - \boldsymbol{\mu}) \right\}. \quad (5)$$

	Gaussian	Generalized Gaussian	Student-t	W-distribution	K-distribution
$g(t)$	$\exp(-t)$	$\exp(-t^s/b) \ s, b > 0$	$(1 + t/d)^{-(d+p)} \ d > 0$	$t^{s-1} \exp(-t^s/b) \ s, b > 0$	$\sqrt{t}^{\nu-p} K_{\nu-p}(2\sqrt{\nu t}) \ \nu > 0$
$\mathfrak{C}_{p,g}$	$\pi^{-p}$	$\frac{s\Gamma(p)b^{-p/s}}{\pi^p\Gamma(p/s)}$	$\frac{\Gamma(p+d)}{\pi^m d^p \Gamma(d)}$	$\frac{s\Gamma(p)b^{-(p+s-1)/s}}{\pi^p\Gamma((p+s-1)/s)}$	$2 \frac{\nu^{(\nu+p)/2}}{\pi^p\Gamma(\nu)}$

[Ollila et al., 2012] proposed to use elliptical distributions for modelling the clutter of HR SAR images:

$$\mathbf{x}_k^t \sim \mathbb{CE}(\mathbf{0}_p, g, \boldsymbol{\Sigma}_t).$$

# Some attempts using Robust estimation theory i

In [Formont et al., 2011], it was proposed to bootstrap the Gaussian GLRT using the Tyler's estimator. If we have  $N$  observations  $\{\mathbf{x}_1, \dots, \mathbf{x}_N\}$  such that  $\mathbf{x}_k \sim \mathbb{C}\mathcal{E}(g, \mathbf{0}_p, \Sigma)$  where:

$$\Sigma = \tau \xi,$$

where  $\text{Tr}(\xi) = p$ .

An estimator of  $\xi$  is:

## Tyler estimator

$$\hat{\xi}_t^{\text{TE}} = \frac{p}{N} \sum_{k=1}^N \frac{\mathbf{x}_k^t \mathbf{x}_k^{tH}}{\mathbf{x}_k^{tH} \{\hat{\xi}_t^{\text{TE}}\}^{-1} \mathbf{x}_k^t}.$$

## Some attempts using Robust estimation theory ii

The test statistic proposed is:

$$\hat{\Lambda}_{G,TE} = \frac{\left| 0.5(\hat{\xi}_1^{TE} + \hat{\xi}_2^{TE}) \right|^N}{\left| \hat{\xi}_1^{TE} \right|^{\frac{N}{2}} \left| \hat{\xi}_2^{TE} \right|^{\frac{N}{2}}} \begin{matrix} H_1 \\ \gtrless \\ H_0 \end{matrix} \lambda$$

### Problems

- The statistic is no longer CFAR matrix due to normalisation :  $\text{Tr}(\hat{\xi}_t^{TE}) = p$ .
- It omits the relative scale between the matrices.

→ We need new statistics taking into account those aspect at the design stage !

# Attempt of GLRT under $\mathbb{CE}$ model

Rather than a 2-step methodology, let's compute the GLRT directly:

**(proposed in Chapter 3)** Detection test:  $\theta_t = \Sigma_t$  &  $\Phi_t = \emptyset$

## Problem

We need to know the density generator  $g$  entirely in order to use the statistic. For most applications,  $g$  is **unknown** and we can't guarantee that it stays the same over time.

# Partial solution

## Idea

Consider the normalized observations:  $\{\mathbf{z}_k^t = \mathbf{x}_k^t / \|\mathbf{x}_k^t\|_2 | 1 \leq k \leq N, 1 \leq t \leq T\}$ . They are known to be  $\mathbb{CAE}$  distributed.

If  $\mathbf{x} \sim \mathbb{CE}(\mathbf{0}_p, g, \tau \boldsymbol{\xi})$  with  $\text{Tr}(\boldsymbol{\xi}) = p$ . Then the PDF of  $\mathbf{z}$  is:

$$p_{\mathbf{z}}^{\mathbb{CAE}}(\mathbf{z}; \boldsymbol{\xi}) = \mathfrak{S}_p^{-1} |\boldsymbol{\xi}|^{-1} (\mathbf{z}^H \boldsymbol{\xi}^{-1} \mathbf{z})^{-p}. \quad (6)$$

**(proposed)** Detection test:  $\boldsymbol{\theta} = \boldsymbol{\xi}_t \quad \& \quad \Phi_t = \emptyset$

# GLRT under $\mathbb{CAE}$ model

The derivation of the GLRT leads to the following result:

## Proposition

$$\hat{\Lambda}_{\mathbb{CAE}} = \frac{\left| \hat{\boldsymbol{\xi}}_0^{\text{TE}} \right|^{TN}}{\prod_{t=1}^T \left| \hat{\boldsymbol{\xi}}_t^{\text{TE}} \right|^N} \prod_{k=1}^N \prod_{t=1}^T \frac{\left( q(\hat{\boldsymbol{\xi}}_0^{\text{TE}}, \mathbf{x}_k^t) \right)^p}{\left( q(\hat{\boldsymbol{\xi}}_t^{\text{TE}}, \mathbf{x}_k^t) \right)^p} \stackrel{\text{H}_1}{\gtrless} \lambda, \quad (7)$$

where:  $\hat{\boldsymbol{\xi}}_t^{\text{TE}} = f_t^{\text{TE}}(\hat{\boldsymbol{\xi}}_t^{\text{TE}})$ ,  $\hat{\boldsymbol{\xi}}_0^{\text{TE}} = \frac{1}{T} \sum_{t=1}^T f_t^{\text{TE}}(\hat{\boldsymbol{\xi}}_0^{\text{TE}})$ ,  $q(\boldsymbol{\xi}, \mathbf{x}) = \mathbf{x}^H \boldsymbol{\xi}^{-1} \mathbf{x}$  and

$$f_t^{\text{TE}}(\boldsymbol{\xi}) = \frac{p}{N} \sum_{k=1}^N \frac{\mathbf{x}_k^t \mathbf{x}_k^{tH}}{q(\boldsymbol{\xi}, \mathbf{x}_k^t)}. \quad (8)$$

# Properties

## Convergence of fixed-point estimates

The algorithm  $[\hat{\xi}_0^{\text{TE}}]_{(i+1)} = \begin{cases} \mathbf{I}_p & \text{if } i = 0 \\ \frac{1}{T} \sum_{t=1}^T f_t^{\text{TE}} \left( [\hat{\xi}_0^{\text{TE}}]_{(i)} \right) & \text{otherwise} \end{cases}$  always converges under some regularity conditions.

Proof: Tyler estimator's convergence is well studied [Kent and Tyler, 1988, Pascal et al., 2008].

## CFARness

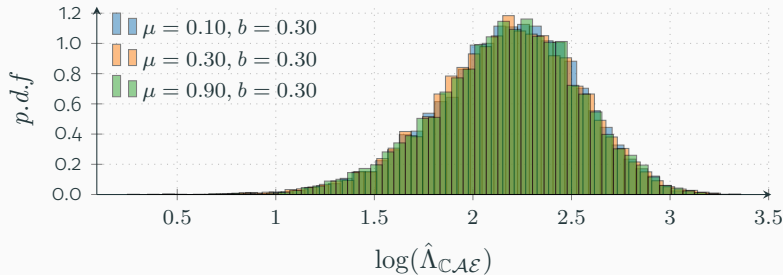
$\hat{\Lambda}_{\mathbb{CAE}}$  is CFAR towards the shape matrix parameter under any  $\mathbb{CE}$  distribution.

Proof: The test statistic is invariant for the group of transformation

$$\mathcal{G} = \left\{ \mathbf{G} \mathbf{z}_k^{(t)} \mid t \in \llbracket 1, T \rrbracket, k \in \llbracket 1, N \rrbracket, \mathbf{G} \in \mathbb{S}_{\mathbb{H}}^p \right\}.$$

## Robust behaviour: Experimental results

In simulation:  $\mathbf{x}_k^t = \sqrt{\tau_k^t} \mathbf{z}_k^t$  where  $\mathbf{z}_k^t \sim \mathcal{CN}(\mathbf{0}_p, (0.5^{|i-j|})_{ij})$  and  $\tau_k^t \sim \Gamma(\mu, b)$  with  $p = 3$ ,  $N = 10$ ,  $T = 3 \cdot 10^4$  Monte-Carlo trials.



### Problem

We still have discarded the **scale** information !

# Deterministic compound-Gaussian modelling i

## Definition

A set of vectors  $\{\mathbf{x}_1, \dots, \mathbf{x}_N\} \in \mathbb{C}^{p \times N}$  is said to follow a deterministic compound-Gaussian model with texture parameter  $\boldsymbol{\tau} = [\tau_1, \dots, \tau_N]^T$  and shape matrix parameter  $\boldsymbol{\xi} \in \mathbb{S}_{\mathbb{H}}^p$  with  $\text{Tr}(\boldsymbol{\xi}) = p$ , denoted  $\mathbb{CCG}(\boldsymbol{\tau}, \boldsymbol{\xi})$  if each observation is distributed as follows:

$$\mathbf{x}_k \sim \mathbb{CN}(\mathbf{0}_p, \tau_k \boldsymbol{\xi}) \quad (9)$$

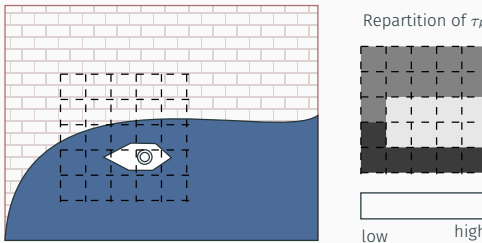
This model is often found in radar applications

[Greco and De Maio, 2016, Pascal et al., 2004]. In the context of SAR ITS we can use the following formulation:

$$\mathbf{x}_k^t \sim \mathbb{CCG}(\boldsymbol{\tau}_t, \boldsymbol{\xi}_t).$$

# Deterministic compound-Gaussian modelling ii

Intuition behind texture:



**(proposed)** Detection tests: 
$$\left\{ \begin{array}{ll} \theta_t = \{\tau_t, \xi_t\} & \& \Phi_t = \emptyset \\ \theta_t = \{\xi_t\} & \& \Phi_t = \{\tau_t\} \text{(equivalent to CAE)} \\ \theta_t = \{\tau_t\} & \& \Phi_t = \{\xi_t\} \end{array} \right.$$

# GLRT for shape matrix and texture ( $\theta_t = \{\tau_t, \xi_t\}$ & $\Phi_t = \emptyset$ )

## Proposition

$$\hat{\Lambda}_{\text{MT}} = \frac{\left| \hat{\boldsymbol{\xi}}_0^{\text{MT}} \right|^{TN}}{\prod_{t=1}^T \left| \hat{\boldsymbol{\xi}}_t^{\text{TE}} \right|^N} \prod_{k=1}^N \frac{\left( \sum_{t=1}^T q\left(\hat{\boldsymbol{\xi}}_0^{\text{MT}}, \mathbf{x}_k^t\right) \right)^{Tp}}{T^{Tp} \prod_{t=1}^T \left( q\left(\hat{\boldsymbol{\xi}}_t^{\text{TE}}, \mathbf{x}_k^t\right) \right)^p} \stackrel{H_1}{\gtrless} \lambda, \quad (10)$$

where:

$$\hat{\boldsymbol{\xi}}_0^{\text{MT}} = \hat{f}_{N,T}^{\text{MT}}\left(\hat{\boldsymbol{\xi}}_0^{\text{MT}}\right) = \frac{p}{N} \sum_{k=1}^N \frac{\sum_{t=1}^T \mathbf{x}_k^t (\mathbf{x}_k^t)^H}{\sum_{t=1}^T q\left(\hat{\boldsymbol{\xi}}_0^{\text{MT}}, \mathbf{x}_k^t\right)}. \quad (11)$$

# GLRT for texture only ( $\theta_t = \{\tau_t\}$ & $\Phi_t = \xi_t$ )

## Proposition

$$\hat{\Lambda}_{\text{Tex}} = \prod_{t=1}^T \frac{\left| \hat{\boldsymbol{\xi}}_t^{\text{Tex}} \right|^N}{\left| \hat{\boldsymbol{\xi}}_t^{\text{TE}} \right|^N} \prod_{k=1}^N \frac{\left( \sum_{t=1}^T q\left(\hat{\boldsymbol{\xi}}_t^{\text{Tex}}, \mathbf{x}_k^t\right) \right)^{Tp}}{T^{Tp} \prod_{t=1}^T \left( q\left(\hat{\boldsymbol{\xi}}_t^{\text{TE}}, \mathbf{x}_k^t\right) \right)^p} \stackrel{H_1}{\gtrless} \lambda, \quad (12)$$

where:

$$\hat{\boldsymbol{\xi}}_t^{\text{Tex}} = f_{N,T,t}^{\text{Tex}} \left( \hat{\boldsymbol{\xi}}_1^{\text{Tex}}, \dots, \hat{\boldsymbol{\xi}}_T^{\text{Tex}} \right) = \frac{Tp}{N} \sum_{k=1}^N \frac{\mathbf{x}_k^t (\mathbf{x}_k^t)^H}{\sum_{t'=1}^T q\left(\hat{\boldsymbol{\xi}}_{t'}^{\text{Tex}}, \mathbf{x}_k^t\right)}. \quad (13)$$

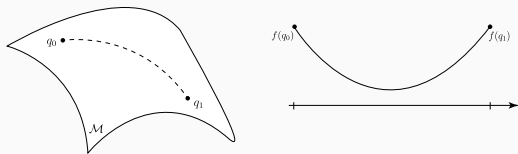
→ We proposed an alternate fixed-point implementation for this estimator.

# Properties: convergence of estimates

## Global maxima

$\hat{\xi}_0^{\text{MT}}$  (resp.  $\hat{\xi}_t^{\text{Tex}}$ ) is the argument to the global maxima of the deterministic compound-Gaussian likelihood under  $H_0$  of problem  $\boldsymbol{\theta}_t = \{\boldsymbol{\tau}_t, \boldsymbol{\xi}_t\} \& \Phi_t = \emptyset$  (resp.  $\boldsymbol{\theta}_t = \{\boldsymbol{\tau}_t\} \& \Phi_t = \{\boldsymbol{\xi}_t\}$ ).

Proof: Using g-convexity on the manifold  $\mathcal{M} = \mathbb{S}_{\mathbb{H}}^p$  as studied in [Wiesel, 2012].



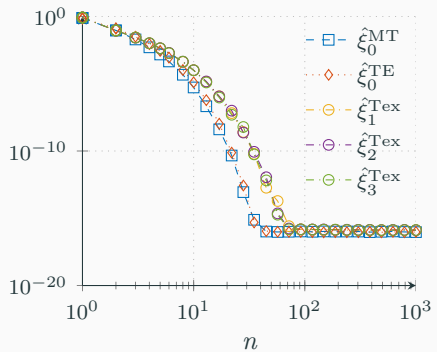
- + We showed that a fixed-point algorithm implementation of  $\hat{\xi}_0^{\text{MT}}$  converges under some minor regularity conditions.

## Experimental validation of convergence

In simulation:  $\mathbf{x}_k^t = \sqrt{\tau_k^t} \mathbf{z}_k^t$  where  $\mathbf{z}_k^t \sim \mathcal{CN}\left(\mathbf{0}_p, (\rho_t^{|i-j|})_{ij}\right)$  and  $\tau_k^t \sim \Gamma(0.3, 0.1)$

with  $p = 3$ ,  $N = 10$ ,  $T = 3 \cdot 10^4$  Monte-Carlo trials.

$\rho_1 = 0.08$ ,  $\rho_2 = 0.9$ ,  $\rho_3 = 0.1$ .

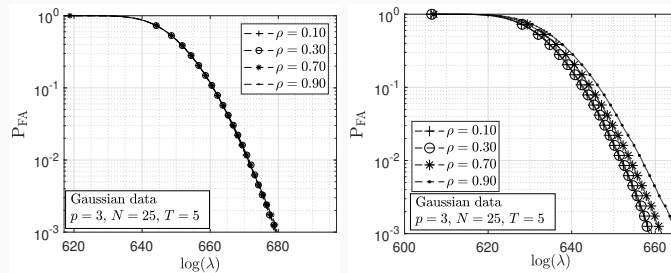


# Properties: CFARness

## CFARness towards shape matrix

$\hat{\Lambda}_{MT}$  is CFAR matrix while  $\hat{\Lambda}_{Tex}$  is not due to trace normalization.

Simulation:  $\mathbf{x}_k^t \sim \mathbb{C}\mathcal{N}(\mathbf{0}_p, (\rho^{|i-j|})_{ij})$ .

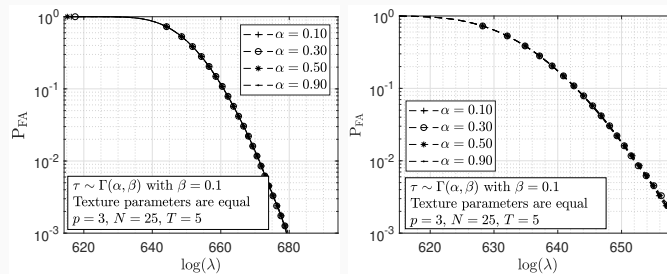


# Properties: CFARness

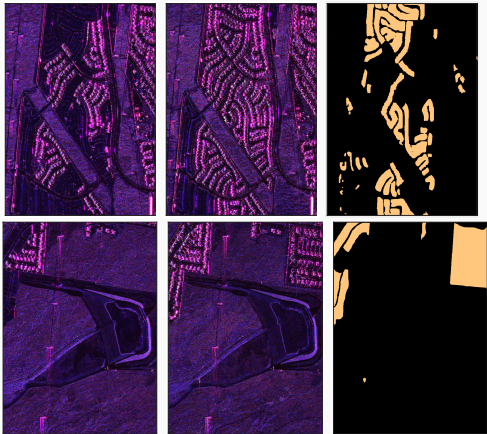
## CFARness towards texture parameters

$\hat{\Lambda}_{\text{MT}}$  and  $\hat{\Lambda}_{\text{Tex}}$  are CFAR texture.

Simulation:  $\mathbf{x}_k^t = \sqrt{\tau_k^t} \mathbf{z}_k^t$  where  $\mathbf{z}_k^t \sim \mathbb{C}\mathcal{N}(\mathbf{0}_p, (0.3^{|i-j|})_{ij})$  and  $\forall(k, t), \tau_k^t = \tau_k$



# Application to real SAR data: UAVSAR (NASA) dataset

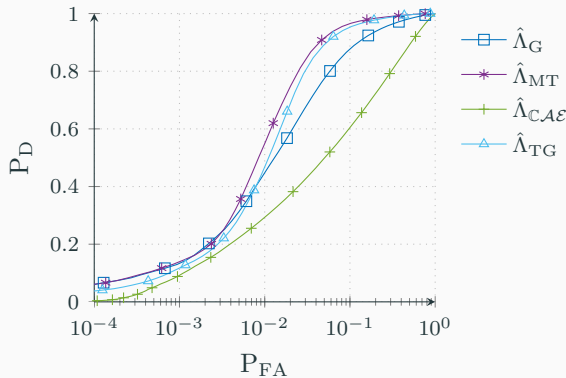
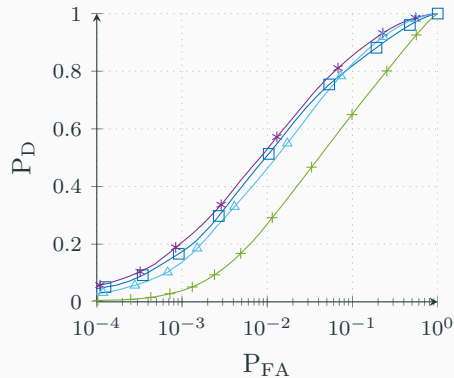


## Data description:

- Polarimetric data:  $p = 3$
- Dimensions: 2360px 600px
- Resolution: 1.67 m (Range) and 0.60 m (Azimuth)

# ROC: UAVSAR

Left: Scene 1. Right: Scene 2.



# Concluding remarks

## What we have achieved

- Robust shape matrix testing under  $\mathbb{CE}$  modelling.
- Robust scale and shape matrix testing under  $\mathbb{CCG}$  modelling.  
→ Improved performance for real SAR images

## Other things to consider

Performance of detection improves when  $p$  increases (diversity) [Mian et al., 2017].

### Drawback:

- $N$  has to be bigger as well !
- No spatial change hypothesis is challenged.

**Solutions:** Regularisation or consider structured matrices.

# Contents of the presentation

## 1 Introduction

- Motivations
- Data

## 2 Change detection based on a statistical framework

- The problem
- State of the art

## 3 Robust Covariance homogeneity testing for Change Detection

- Tests using Complex Elliptical Symmetric distributions
- Tests using deterministic compound-Gaussian modelling

## 4 Tests using Low-rank models

## 5 Clustering SAR ITS with Riemannian geometry: an opening

## 6 Conclusions

# Low-rank models

## Gaussian context

$\mathbf{x} \sim \mathbb{C}\mathcal{N}(\mathbf{0}_p, \Sigma_t + \sigma^2 \mathbf{I})$  where  $\text{rank}(\Sigma_t) = R < p$ .

$$\theta_t = \Sigma_t \quad \& \quad \Phi_t = \emptyset.$$

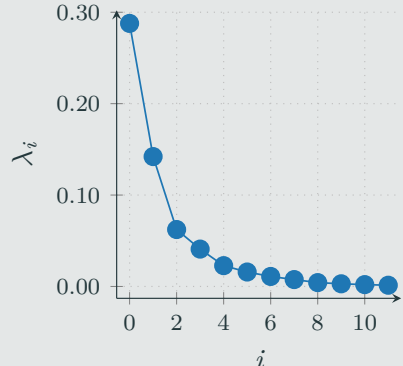
## CCG context

Assuming  $\mathbf{x} \sim \mathbb{C}\mathcal{CG}(\tau_t, \xi_t + \sigma^2 \mathbf{I})$  where  $\text{rank}(\xi_t) = R < p$ .

$$\theta_t = \{\tau_t, \xi_t\} \quad \& \quad \Phi_t = \emptyset.$$

Work done in collaboration with **Rayen Ben Abdallah** and **Arnaud Breloy** of LEME, Paris Nanterre University.

## Spectrum of UAVSAR data (wavelets)



# Optimization considerations: Gaussian case ( $\theta_t = \Sigma_t$ & $\Phi_t = \emptyset$ )

## Expression of the GLRT: no closed form

$$\hat{\Lambda}_{\text{LRG}} = \frac{\mathcal{L}\left(\mathbb{W}_{1,T}/H_1; \mathcal{T}_R\{\hat{\Sigma}_1\}, \dots, \mathcal{T}_R\{\hat{\Sigma}_T\}\right)}{\mathcal{L}\left(\mathbb{W}_{1,T}/H_0; \mathcal{T}_R\{\hat{\Sigma}_0\}\right)} \stackrel{H_1}{\gtrless} \lambda. \quad (14)$$

where  $\hat{\Sigma}_t = \frac{1}{N} \sum_{k=1}^N \mathbf{x}_k^t (\mathbf{x}_k^t)^H$  and for  $\Sigma \stackrel{\text{EVD}}{=} \mathbf{V} \boldsymbol{\Lambda} \mathbf{V}^H$ ,  $\mathcal{T}_R\{\Sigma\} \stackrel{\text{EVD}}{=} \mathbf{V} \tilde{\boldsymbol{\Lambda}} \mathbf{V}^H$  with

$$[\tilde{\boldsymbol{\Lambda}}]_{i,i} = \begin{cases} \max([\boldsymbol{\Lambda}]_{i,i}, \sigma^2) & i \leq R \\ \sigma^2 & i > R \end{cases} \quad (15)$$

## Optimization considerations: CCG case ( $\theta_t = \{\tau_t, \xi_t\}$ & $\Phi_t = \emptyset$ )

Same methodology for this case but the optimization of the likelihood is **non-convex**. We propose the following approach:

### Low-rank Compound-Gaussian GLRT

$$\hat{\Lambda}_{LRCG} = \frac{\mathcal{L}\left(\mathbb{W}_{1,T}/H_1 ; \left\{\{\hat{\xi}_t\}, \{\hat{\tau}_k^t\}\right\}\right)}{\mathcal{L}\left(\mathbb{W}_{1,T}/H_0 ; \left\{\hat{\xi}_0, \{\hat{\tau}_k^0\}\right\}\right)} \stackrel{H_1}{\gtrless} \lambda.$$

where the set of parameters  $\hat{\xi}_0, \hat{\xi}_t, \tau_k^t, \tau_k^0$  are estimated through a block Majorization-Minimization of the negative log-likelihood.  
→ Convergence insured to a local optima.

# Optimization for $\mathcal{CCG}$ case

---

**Algorithm 1** BCD for MLEs under  $H_1$ 

Initialise  $\boldsymbol{\xi}_t = \mathbf{I}_p$

**repeat**

$$\tau_k^t = ((\mathbf{x}_k^t)^H \boldsymbol{\Sigma}_t^{-1} \mathbf{x}_k^t) / p$$

$$\boldsymbol{\xi}_t = \mathcal{T}_R \left\{ \frac{1}{N} \sum_{k=1}^K \frac{\mathbf{x}_k^t (\mathbf{x}_k^t)^H}{\tau_k^t} \right\}$$

**until** convergence

**Output:**  $\left\{ \hat{\boldsymbol{\xi}}_t, \{\hat{\tau}_k^t\} \right\}$

---

---

**Algorithm 2** BCD for MLE under  $H_0$ 

Initialise  $\boldsymbol{\xi}_0 = \mathbf{I}_p$

**repeat**

$$\tau_k^0 = \left( \sum_{t=1}^T (\mathbf{x}_k^t)^H \boldsymbol{\Sigma}_0^{-1} \mathbf{x}_k^t \right) / Tp$$

$$\boldsymbol{\xi}_0 = \mathcal{T}_R \left\{ \frac{1}{N} \sum_{k=1}^N \sum_{t=1}^T \frac{\mathbf{x}_k^1 (\mathbf{x}_k^1)^H}{T\tau_k^0} \right\}$$

**until** convergence

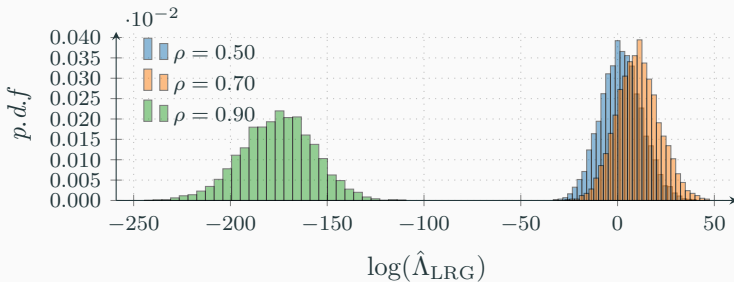
**Output:**  $\left\{ \hat{\boldsymbol{\xi}}_0, \{\hat{\tau}_k^0\} \right\}$

---

# CFARness: Gaussian case

**Simulation setup:**  $p = 20, N = 50, T = 10, R = 5$

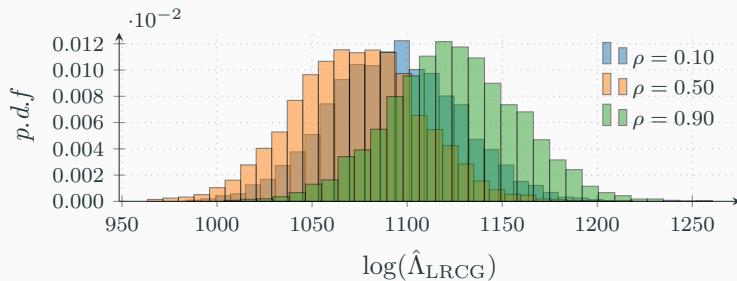
$\mathbf{x}_k^t \sim \mathbb{C}\mathcal{N}(\mathbf{0}_p, \mathcal{T}_R\{(\rho^{|i-j|})_{ij}\})$  with  $10^4$  Monte-Carlo trials.



# CFARness: $\mathcal{CCG}$ case

**Simulation setup:**  $p = 20, N = 50, T = 10, R = 5$

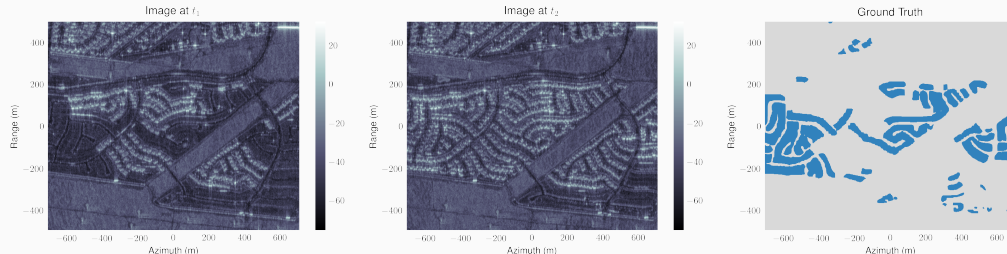
$\mathbf{x}_k^t \sim \mathbb{C}\mathcal{N}(\mathbf{0}_p, \mathcal{T}_R\{(\rho^{|i-j|})_{ij}\})$  with  $10^4$  Monte-Carlo trials.



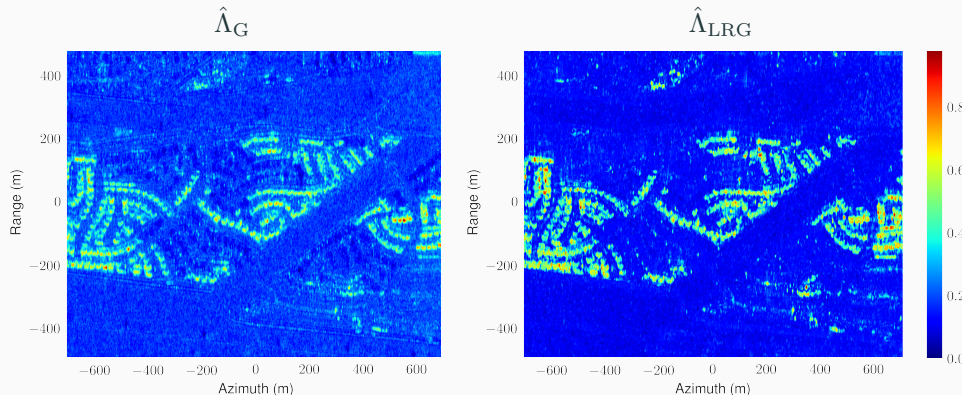
# Experimental results: Dataset

## Description

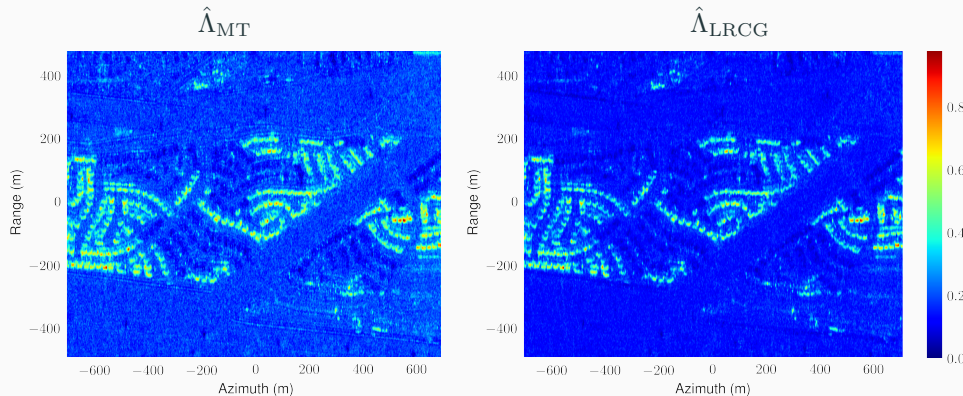
- Polarimetric data → wavelet decompr. [Mian et al., 2017] →  $p = 12$  dim. pixels
- Image size: 2360px×600px
- Resolution: 1.67 m (Range) and 0.60 m (Azimuth)
- CD ground truth from [Nascimento et al., 2019]



# Results with a $5 \times 5$ sliding windows: Gaussian detectors



# Results with a $5 \times 5$ sliding windows: Robust detectors



## Performance curves

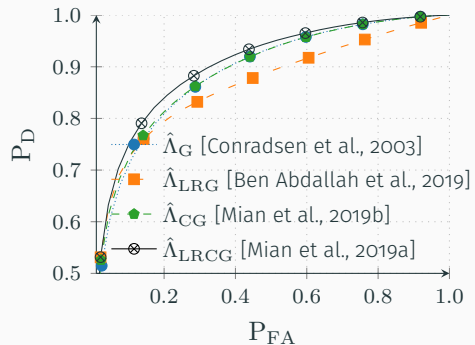


**Figure 4:** Probability of detection  $P_D$  versus probability of false alarm  $P_{FA}$  with  $(p = 12, N = 25, R = 3)$

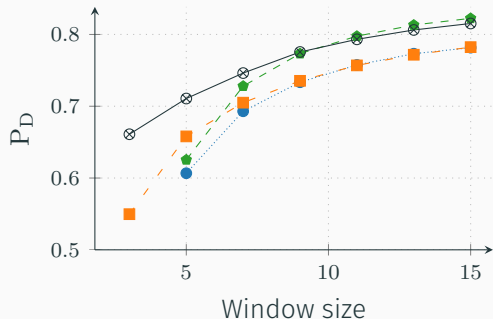


**Figure 5:**  $P_D$  versus the size of window at  $P_{FA} = 5\%$  with  $(p = 12, R = 3)$

# Concluding remarks and perspectives

## Conclusions

We have tests assuming low-rank structure of the matrix that:

- Reduced considerably the number of false alarms.
- perform well with lower window size.

## Perspectives

- Rank estimation strategies [Stoica and Selen, 2004, Terreux et al., 2018]
- CFAR test statistic in Low-rank ?  
→ Random Matrix theory correction [Vallet et al., 2019].
- Other structures: Persymmetry, Toeplitz, etc

# Contents of the presentation

## 1 Introduction

- Motivations
- Data

## 2 Change detection based on a statistical framework

- The problem
- State of the art

## 3 Robust Covariance homogeneity testing for Change Detection

- Tests using Complex Elliptical Symmetric distributions
- Tests using deterministic compound-Gaussian modelling

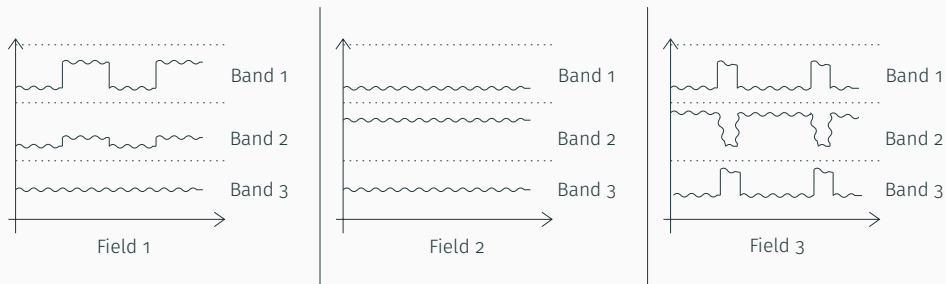
## 4 Tests using Low-rank models

## 5 Clustering SAR ITS with Riemannian geometry: an opening

## 6 Conclusions

# Example of series

# Illustrative example



# The SAR ITS clustering problem

**Problem:** Can we cluster pixels according to their temporal evolution ?

- Pattern of changes
- Type of objects who change

## Idea

Consider a time-series clustering problem !

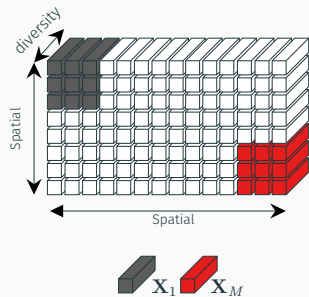
**We need:** a **feature** to represent the time series and a **distance**.

Work done in collaboration with **Florent Bouchard** of University Savoie Mont-Blanc.

# K-means algorithm

→ We need a descriptive feature and a distance on the feature space !

# Multivariate SAR clustering: state of the art



**Spatial clustering:** cluster patches  $\{\mathbf{X}_i | 1 \leq i \leq M\}$  where each set is defined as  $\mathbf{X}_i = \{\mathbf{x}_k \in \mathbb{C}^p | 1 \leq k \leq N\}$

## Wishart Classifier ([Jong-Sen Lee et al., 1999])

**Feature:**  $\hat{\Sigma} = N^{-1} \sum_{k=1}^N \mathbf{x}_k \mathbf{x}_k^H$ .

$$d_W(\Sigma, C) = \log |\mathbf{C}| - \log |\Sigma| + \text{tr}(\mathbf{C}^{-1} \Sigma) \quad (16)$$

## Robust distance [Vasile et al., 2010]

**Feature:** Tyler estimator.

$$d_{SIRV}(\Sigma, C) = \log |\mathbf{C}| - \log |\Sigma| + \frac{p}{N} \sum_{k=1}^N \frac{q(\mathbf{C}, \mathbf{x}_k)}{q(\Sigma, \mathbf{x}_k)} \quad (17)$$

# Clustering on temporal features

$\{\mathbf{X}_i | 1 \leq i \leq N\}$  where each set  
 $\mathbf{X}_i = \{\mathbf{x}^t \in \mathbb{C}^p | 1 \leq t \leq T\}$

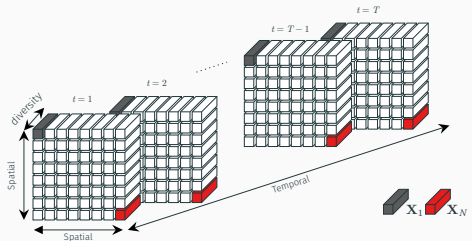
## Temporal features

$$\theta = \{\hat{\xi}^{\text{TE}}, \hat{\tau}\},$$

where

$$\hat{\xi}^{\text{TE}} = \frac{p}{N} \sum_{t=1}^T \frac{\mathbf{x}^t (\mathbf{x}^t)^H}{(\mathbf{x}^t)^H \{\hat{\xi}^{\text{TE}}\}^{-1} (\mathbf{x}^t)},$$

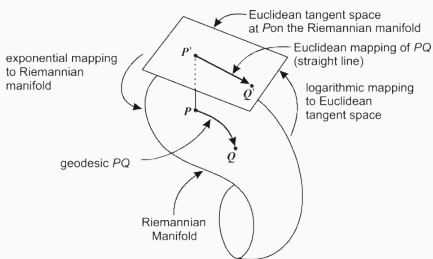
$$\hat{\tau} = p^{-1} (\mathbf{x}^t)^H \{\hat{\xi}^{\text{TE}}\}^{-1} (\mathbf{x}^t)$$



→ We need a distance !

# Riemannian Geometry for clustering

We consider **Riemannian Geometry** on the manifold



**Credit:** [Gao and Harrison, 2016]

$$\mathcal{M}_{p,T} = \mathbb{S}_{\mathbb{H},|\bullet|}^p \times (\mathbb{R}^+)^T,$$

$$\text{where } \mathbb{S}_{\mathbb{H},|\bullet|}^p = \{\xi \in \mathbb{S}_{\mathbb{H}}^p \mid |\xi| = 1\}.$$

Riemannian framework have been shown to be useful for clustering when the feature lie in a manifold [Formont et al., 2011, Berthoumieu et al., 2017].

## Problem

We have to develop the geometry on this new manifold !

# Natural distance (from Fisher Information Metric)

## Proposition

The natural distance between two points  $\boldsymbol{\theta}_0 = (\boldsymbol{\xi}_0, \boldsymbol{\tau}_0)$  and  $\boldsymbol{\theta}_1 = (\boldsymbol{\xi}_1, \boldsymbol{\tau}_1)$  belonging to  $\mathcal{M}_{p,N}$  is given by:

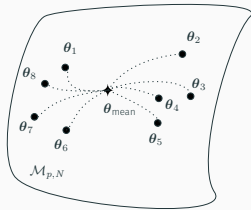
$$\delta_{\mathcal{M}_{p,N}}^2 = \delta_{\mathbb{S}_{\mathbb{H}, |\bullet|}^p}^2(\boldsymbol{\xi}_0, \boldsymbol{\xi}_1) + \delta_{(\mathbb{R}^+)^N}^2(\boldsymbol{\tau}_0, \boldsymbol{\tau}_1). \quad (18)$$

where:

$$\begin{aligned} \delta_{\mathbb{S}_{\mathbb{H}}^p}^2(\boldsymbol{\xi}_0, \boldsymbol{\xi}_1) &= \|\log(\boldsymbol{\xi}_0^{-\frac{1}{2}} \boldsymbol{\xi}_1 \boldsymbol{\xi}_0^{-\frac{1}{2}})\|_2^2. \\ \delta_{(\mathbb{R}^+)^N}^2(\boldsymbol{\tau}_0, \boldsymbol{\tau}_1) &= \|\log(\boldsymbol{\tau}_0^{-1} \odot \boldsymbol{\tau}_1)\|_2^2. \end{aligned} \quad (19)$$

→ No crossed term between shape matrix and texture part ! (choice of normalization)

# Mean on $\mathcal{M}_{p,N}$



## Riemannian mean

$$\boldsymbol{\theta}_{\text{mean}} = \operatorname{argmin}_{\boldsymbol{\theta} \in \mathcal{M}_{p,N}} \sum_{m=1}^M \delta_{\mathcal{M}_{p,N}}^2(\boldsymbol{\theta}, \boldsymbol{\theta}_m)$$

Can be done separately:

- Concerning  $\mathbb{S}_{\mathbb{H}, |\bullet|}^p$ , no closed-form [Moakher, 2005]:

$$\boldsymbol{\xi}_{\text{mean}} = \operatorname{argmin}_{\boldsymbol{\xi} \in \mathbb{S}_{\mathbb{H}, |\bullet|}^p} \sum_{m=1}^M \delta_{\mathbb{S}_{\mathbb{H}, |\bullet|}^p}^2(\boldsymbol{\xi}, \boldsymbol{\xi}_m).$$

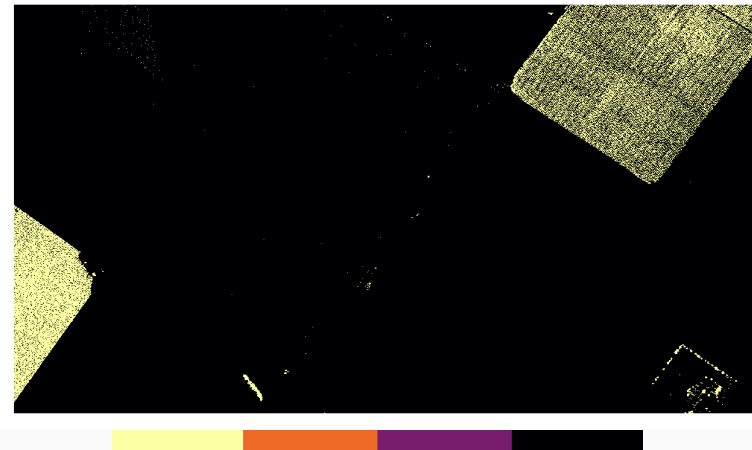
- Concerning  $(\mathbb{R}^+)^N$ , the geometric mean is:

$$\boldsymbol{\tau}_{\text{mean}} = \left( \odot_{m=1}^M \boldsymbol{\tau}_m \right)^{1/M}.$$

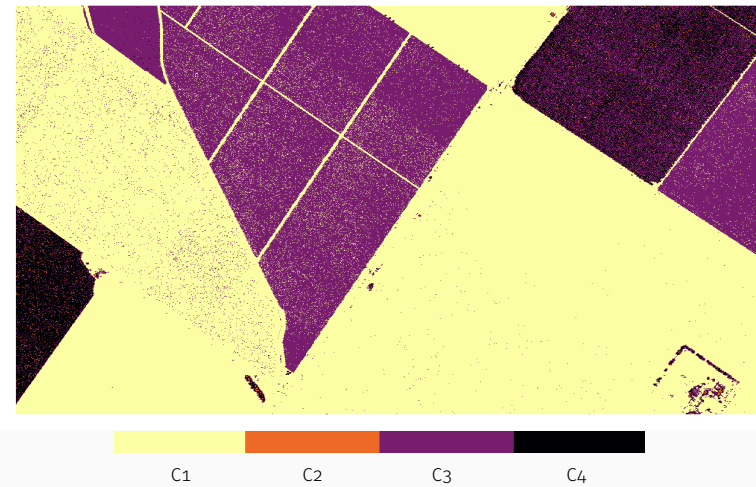
# Application to SAR data

UAVSAR data (Courtesy NASA/JPL-Caltech): polarimetry ( $p = 3$ ) and  $T = 17$  images.

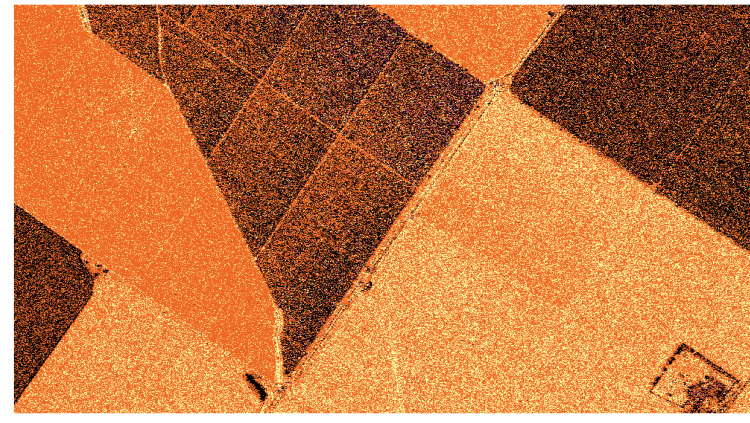
# Wishart Classifier



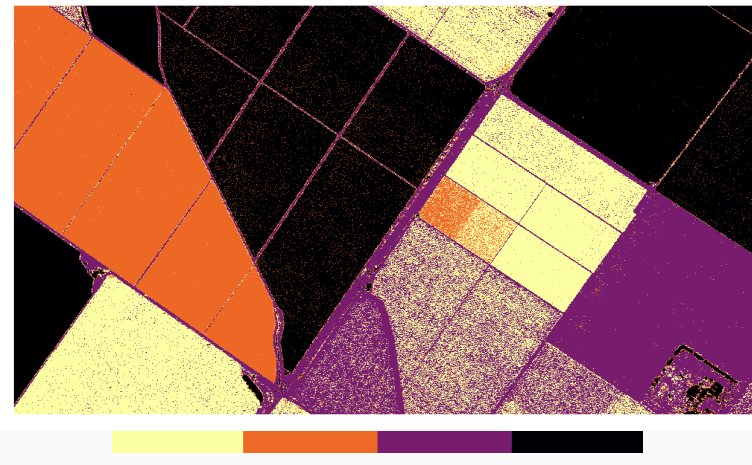
# Wishart Classifier with Riemannian mean



# SIRV distance with Riemannian mean



# CCG Riemannian distance and mean



# Contents of the presentation

## 1 Introduction

- Motivations
- Data

## 2 Change detection based on a statistical framework

- The problem
- State of the art

## 3 Robust Covariance homogeneity testing for Change Detection

- Tests using Complex Elliptical Symmetric distributions
- Tests using deterministic compound-Gaussian modelling

## 4 Tests using Low-rank models

## 5 Clustering SAR ITS with Riemannian geometry: an opening

## 6 Conclusions

# Conclusions of the Ph.d

## What we have done

- Found a way to construct diversity in monovariate HR SAR images
- Improved change detection algorithms for multivariate HR SAR images
- Considered change-point estimation problems as well
- Developed a framework for Riemannian clustering of time series (still working on it)

## Several collaborations

- with **Lucien Bacharach** of SATIE, ENS Paris-Saclay and **Alexandre Renaux** of L2S, CentraleSupélec, on lower bounds for change-point
- with **Rayen Ben Abdallah** and **Arnaud Breloy** of LEME, Paris Nanterre on low-rank change detection
- with **Florent Bouchard** of LISTIC, Université Savoie Mont-Blanc on Robust Riemannian clustering
- with **Jialun Zhou, Salem Said and Yannick Berthomieu** of IMS, Bordeaux on Riemannian stochastic optimization

# Perspectives of the Ph.d

## Change detection and change-point estimation

- Consider others structures and improve current test statistics.
- Integrate temporal or spatial correlation in the design:
  - Typically done in Finance applications
- Improve lower-bound to take into account non-Gaussian modelling.

## Time series clustering

- Validate current methodology
- Consider a multivariate Dynamic Time Warping (DTW) framework
- Consider distance between segments on manifolds

**Thanks for your attention !**

# List of publications: i

## Journals :

- **A. Mian**, G. Ginolhac, J. Ovarlez and A. M. Atto, "New Robust Statistics for Change Detection in Time Series of Multivariate SAR Images", in IEEE Transactions on Signal Processing, vol. 67, no. 2, pp. 520-534, 15 Jan, 2019.
- **A. Mian**, J. Ovarlez, A. M. Atto and G. Ginolhac, "Design of New Wavelet Packets Adapted to High-Resolution SAR Images With an Application to Target Detection," in IEEE Transactions on Geoscience and Remote Sensing, vol. 57, no. 6, pp. 3919-3932, June 2019.
- R. Ben Abdallah, **A. Mian**, A. Breloy, A. Taylor, M. N. El Korso and D. Lautru, "Detection Methods Based on Structured Covariance Matrices for Multivariate SAR Images Processing," in IEEE Geoscience and Remote Sensing Letters.
- (In preparation) **A. Mian**, F. Bouchard, G. Ginolhac, J-p. Ovarlez, "Multivariate SAR Data Clustering based on Riemannian Geometry over Robust Models", SIAM Journal of Imaging Science

## List of publications: ii

### Conferences proceedings :

- **A. Mian**, J. P. Ovarlez, G. Ginolhac and A. M. Atto, "Multivariate change detection on high resolution monovariate SAR image using linear time-frequency analysis," 2017 25th European Signal Processing Conference (EUSIPCO), Kos, 2017, pp. 1942-1946.
- **A. Mian**, J. P. Ovarlez, G. Ginolhac, A. M. Atto, Détection de changement sur images SAR monovariées par analyse temps-fréquence linéaire, GRETSI 2017 XXVIème colloque, 2017, Juan-les-Pins.
- **A. Mian**, J. Ovarlez, G. Ginolhac and A. M. Atto, "A Robust Change Detector for Highly Heterogeneous Multivariate Images," 2018 IEEE International Conference on Acoustics, Speech and Signal Processing (ICASSP), Calgary, AB, 2018, pp. 3429-3433.
- **A. Mian**, J. Ovarlez, G. Ginolhac and A. M. Atto, "Robust Detection and Estimation of Change-Points in a Time Series of Multivariate Images," 2018 26th European Signal Processing Conference (EUSIPCO), Rome, 2018, pp. 1097-1101.

## List of publications: iii

- **A. Mian**, L. Bacharach, G. Ginolhac, A. Renaux, M. N. El Korso and J. -. Ovarlez, "Designing Sar Images Change-point Estimation Strategies Using an Mse Lower Bound," ICASSP 2019 - 2019 IEEE International Conference on Acoustics, Speech and Signal Processing (ICASSP), Brighton, United Kingdom, 2019, pp. 5312-5316.
- **A. Mian**, A.Breloy, G. Ginolhac, J.-P. Ovarlez, Robust Low-rank Change Detection for SAR Image Time Series, 2019 International Geoscience, Remote Sensing Symposium (IGARSS), Yokohama, Japan, 2019.

## References i

-  Ben Abdallah, R., Mian, A., Breloy, A., Taylor, A., El Kors, M. N., and Lautru, D. (2019).  
**Detection methods based on structured covariance matrices for multivariate sar images processing.**  
*IEEE Geoscience and Remote Sensing Letters*, 16(7):1160–1164.
-  Berthoumieu, Y., Bombrun, L., Germain, C., and Said, S. (2017).  
**Classification approach based on the product of riemannian manifolds from gaussian parametrization space.**  
In *2017 IEEE International Conference on Image Processing (ICIP)*, pages 206–210.
-  Ciuonzo, D., Carotenuto, V., and Maio, A. D. (2017).  
**On multiple covariance equality testing with application to SAR change detection.**  
*IEEE Transactions on Signal Processing*, 65(19):5078–5091.

## References ii

-  Conradsen, K., Nielsen, A. A., Schou, J., and Skriver, H. (2003).  
**A test statistic in the complex wishart distribution and its application to change detection in polarimetric SAR data.**  
*IEEE Transactions on Geoscience and Remote Sensing*, 41(1):4–19.
-  Formont, P., Ovarlez, J. P., Pascal, F., Vasile, G., and Ferro-Famil, L. (2011).  
**On the extension of the product model in PolSAR processing for unsupervised classification using information geometry of covariance matrices.**  
In *2011 IEEE International Geoscience and Remote Sensing Symposium*, pages 1361–1364.
-  Formont, P., Pascal, F., Vasile, G., Ovarlez, J.-P., and Ferro-Famil, L. (2011).  
**Statistical classification for heterogeneous polarimetric SAR images.**  
*IEEE Journal of Selected Topics in Signal Processing*, 5(3):567–576.

## References iii

-  Gao, K. and Harrison, J. P. (2016).  
**Mean and dispersion of stress tensors using euclidean and riemannian approaches.**  
*International Journal of Rock Mechanics and Mining Sciences*, 85:165 – 173.
-  Greco, M. S. and De Maio, A., editors (2016).  
**Modern Radar Detection Theory.**  
SciTech Publishing.
-  Jong-Sen Lee, Grunes, M. R., Ainsworth, T. L., Li-Jen Du, Schuler, D. L., and Cloude, S. R. (1999).  
**Unsupervised classification using polarimetric decomposition and the complex wishart classifier.**  
*IEEE Transactions on Geoscience and Remote Sensing*, 37(5):2249–2258.

## References iv

-  Kay, S. M. and Gabriel, J. R. (2003).  
**An invariance property of the generalized likelihood ratio test.**  
*IEEE Signal Processing Letters*, 10(12):352–355.
-  Kent, J. T. and Tyler, D. E. (1988).  
**Maximum likelihood estimation for the wrapped cauchy distribution.**  
*Journal of Applied Statistics*, 15(2):247–254.
-  Mian, A., Breloy, A., Ginolhac, G., and Ovarlez, J. (2019a).  
**Robust low-rank change detection for sar image time series.**  
In *2019 IEEE Geoscience and Remote Sensing (IGARSS)*.
-  Mian, A., Ginolhac, G., Ovarlez, J., and Atto, A. M. (2019b).  
**New robust statistics for change detection in time series of multivariate sar images.**  
*IEEE Transactions on Signal Processing*, 67(2):520–534.

## References v

-  Mian, A., Ovarlez, J., Atto, A. M., and Ginolhac, G. (2019c).  
**Design of new wavelet packets adapted to high-resolution sar images with an application to target detection.**  
*IEEE Transactions on Geoscience and Remote Sensing*, 57(6):3919–3932.
-  Mian, A., Ovarlez, J. P., Ginolhac, G., and Atto, A. (2017).  
**Multivariate change detection on high resolution monovariate sar image using linear time-frequency analysis.**  
In *2017 25th European Signal Processing Conference (EUSIPCO)*, pages 1942–1946.
-  Moakher, M. (2005).  
**A differential geometric approach to the geometric mean of symmetric positive-definite matrices.**  
*SIAM Journal on Matrix Analysis and Applications*, 26(3):735–747.

-  Nascimento, A. D. C., Frery, A. C., and Cintra, R. J. (2019).  
**Detecting changes in fully polarimetric SAR imagery with statistical information theory.**  
*IEEE Transactions on Geoscience and Remote Sensing*, 57(3):1380–1392.
-  Ollila, E., Tyler, D. E., Koivunen, V., and Poor, H. V. (2012).  
**Compound-Gaussian clutter modeling with an inverse Gaussian texture distribution.**  
*IEEE Signal Processing Letters*, 19(12):876–879.
-  Pascal, F., Chitour, Y., Ovarlez, J.-P., Forster, P., and Larzabal, P. (2008).  
**Covariance structure maximum likelihood estimates in compound Gaussian noise : Existence and algorithm analysis.**  
*Signal Processing, IEEE Transactions on*, 56(1):34–48.

## References vii

-  Pascal, F., Ovarlez, J.-P., Forster, P., and Larzabal, P. (2004).  
**Constant false alarm rate detection in spherically invariant random processes.**  
In *European Signal Processing Conference (EUSIPCO)*, pages 2143–2146, Vienna.
-  Stoica, P. and Selen, Y. (2004).  
**Model-order selection: a review of information criterion rules.**  
*IEEE Signal Processing Magazine*, 21(4):36–47.
-  Terreaux, E., Ovarlez, J., and Pascal, F. (2018).  
**A toeplitz-tyler estimation of the model order in large dimensional regime.**  
In *2018 IEEE International Conference on Acoustics, Speech and Signal Processing (ICASSP)*, pages 4489–4493.

## References viii

-  Vallet, P., Ginolhac, G., Pascal, F., and Forster, P. (2019).  
**An improved low rank detector in the high dimensional regime.**  
In *ICASSP 2019 - 2019 IEEE International Conference on Acoustics, Speech and Signal Processing (ICASSP)*, pages 5336–5340.
-  Vasile, G., Ovarlez, J., Pascal, F., and Tison, C. (2010).  
**Coherency matrix estimation of heterogeneous clutter in high-resolution polarimetric sar images.**  
*IEEE Transactions on Geoscience and Remote Sensing*, 48(4):1809–1826.
-  Wiesel, A. (2012).  
**Geodesic convexity and covariance estimation.**  
*IEEE Transactions on Signal Processing*, 60(12):6182–6189.